Supporting Information

Hart et al. 10.1073/pnas.1319488111

SI Materials and Methods

Treatment of Human Cells K-562, MOLT-4, HL-60, and SW-480 and Quail Cells with KJ-Pyr-9. For testing adherent cell types, 1.5×10^5 cells were seeded into MP-24 dishes and incubated overnight at 37 °C. The next day, the culture medium was replaced by 200 µL of ECB buffer (135 mM NaCl, 5 mM KCl, 10 mM Hepes, pH 7.4, 1 mM $MgCl_2$, and 1 mM $CaCl_2$) and the KJ-Pyr-9 compound in 25 or 50 µM final concentration (diluted from a stock solution in DMSO). Cells were incubated at 37 °C for 30 min. Then, 800 µL cell-culture medium containing the compound was added and the cells were further incubated for 24 h at 37 °C. For cells grown in suspension (K-562, MOLT-4, and HL-60), 1.5×10^5 cells were collected by centrifugation at $150 \times g$ and resuspended in 200 µL of ECB buffer containing the compound. After a 30-min incubation at 37 °C, 800 µL culture medium containing the compound was added and the cells were incubated as above. Cell micrographs were taken 24 h after treatment with the compound.

Immunofluorescence Staining of NDRG1. Tumor tissues were fixed in 4% paraformaldehyde overnight, dehydrated, and embedded in paraffin. All samples were sectioned at 5 µm. Processing of the sections for protein localization followed the Cell Signaling Immunofluorescence General Protocol. The primary antibody against NDRG1 was from Cell Signaling (5196). Standard immunohistochemistry procedures for polyclonal primary antibodies were applied using instructions from the Cell Signaling Immunofluorescence General Protocol. NDRG1 and nuclear staining were performed using FITC-conjugated goat anti-rabbit IgG (Sigma; F-0382) as secondary antibody and tissue sections were mounted in ProLong Gold Antifade Reagent with DAPI (Molecular Probes; 8961S). Micrographs were taken at 40× magnification (microscope objective) with a Hamamatsu digital CCD camera.

RNA Sequencing. P493-6 cells were seeded at an initial density of 1×10^5 cells per mL in 4 mL medium in a six-well plate. Cells were grown in the presence of 0.1 µg/mL doxycycline, 20 µM KJ-Pyr-9, or a combination of both. Cells were grown for 48 h and isolated by centrifugation at $300 \times g$ for 3 min. Total RNA was prepared using a Maxwell 16 instrument (Promega) with simplyRNA LEV reagents. Life Technologies RiboMinus Kits were used to remove rRNA from total RNA samples. One microgram of total RNA input was used for each sample. RNA sequencing (RNAseq) libraries were prepared from ribodepleted RNA samples using the NEBNext Ultra RNA Library Prep Kit for Illumina, following the manufacturer's protocols. The libraries were sequenced on an Illumina HiSeq 2000 using 100-bp single-ended reads. Raw as well as processed data are available online under Gene Expression Omnibus accession no. GSE58168.

RNAseq Data Analysis. RNAseq was performed on P493-6 cells in triplicate with no treatment, 20 µM KJ-Pyr-9, or 0.1 µg/mL doxycycline. Between 9 and 33 million reads were collected per sample. After filtering at 0.3 counts per million, 12,056 genes could be quantified. The dataset showed a low variance at a biological coefficient of variation of 0.057. Reads were aligned to the HG19/GRCh37 genome using the STAR aligner (1). Reads were counted using htseq (2) using GENCODE v19 gene annotations. Analysis of differential expression was performed using edgeR (3) after filtering the data such that a minimum of three samples had more than 0.3 reads per million. Gene set enrichment analysis was performed using GSEA2 (4) using the MsigDB v4.0 curated gene sets.

1. Dobin A, et al. (2013) STAR: Ultrafast universal RNA-seq aligner. *Bioinformatics* 29(1):15–21.
2. Anders S, Pyl PT, Huber W (2014) HTSeq—A Python framework to work with high-throughput sequencing data. bioRxiv:10.1101/002824.
3. Robinson MD, McCarthy DJ, Smyth GK (2010) edgeR: A Bioconductor package for differential expression analysis of digital gene expression data. *Bioinformatics* 26(1):139–140.
4. Subramanian A, et al. (2005) Gene set enrichment analysis: A knowledge-based approach for interpreting genome-wide expression profiles. *Proc Natl Acad Sci USA* 102(43):15545–15550.

Fig. S1. Fluorescence polarization screen of compound mixtures. Compound mixtures were added at the indicated concentrations to a solution of the MYC basic helix–loop–helix leucine zipper domain. To these, MAX and Alexa Fluor 594-tagged E box-containing DNA duplex was added. Changes in MYC–MAX dimerization influence DNA binding and hence the polarization of Alexa Fluor 594. Fluorescence polarization is presented as % inhibition, where 0% is the DMSO control and 100% is the DNA duplex without protein. Numbers on the abscissa indicate compound mixtures.

Fig. S2. Western blot documenting expression of the larger and smaller isoforms of MYC from the three RCAS constructs used: ATG-MYC, in which the noncanonical upstream CTG start codon is mutated to ATG, wild-type MYC, and CAG-MYC, in which the upstream start codon is mutated to the nonfunctional CAG, restricting production to the small isoform of MYC.

Fig. S3. Effect of KJ-Pyr-9 on the *Renilla* luciferase (*R*luc)-PCA (protein fragment complementation assay)–based MYC$^{332–439}$–MAX biosensor. (*A*) Schematic illustration of the *R*luc-PCA–based biosensor for the analysis and quantification of binary MYC$^{332–439}$–MAX complexes in living cells. (*B*) HEK293 cells transiently expressing the indicated PCA couples were treated for 6 h with 20 μM KJ-Pyr-9. Cell suspensions were then transferred to 96-well plates for bioluminescence analysis. Statistical significance was assessed using a paired Student *t* test (±SEM from four independent experiments and as independent duplicates; *P* values <0.001) applied to the values indicated by the bracket. (*C*) Immunoblot (IB) analyses using anti-*R*luc antibodies show expression levels of the indicated PCA hybrid proteins in cells without or with compound exposure.

Fig. S4. Effect of KJ-Pyr-9 on cell proliferation. (*A*) Cell lines NCI-H460, MDA-MB-231, and SUM-159PT. (*B*) Burkitt lymphoma cell lines Akata, Ramos, and Raji. Error bars represent standard error of the mean (SEM).

Fig. S5. Effect of KJ-Pyr-9 on the proliferation of v-*myc*–transformed quail embryo fibroblasts (*A*) and of human leukemia and carcinoma cell lines (*B*). The compound was added in the indicated concentrations to primary quail embryo fibroblasts (QEFs), quail cell lines transformed by the oncogenes v-*myc* (Q8, QEF/MC29), v-*jun* (VJ), or methylcholanthrene (QT6), human skin fibroblasts (hFBs), the nonadherently growing leukemia cell lines K-562, MOLT-4, or HL-60, or the adenocarcinoma cell line SW-480. As a control, the compound's solvent, DMSO, was added to the cells. Microphotographs were taken 24 h after addition of the compound.

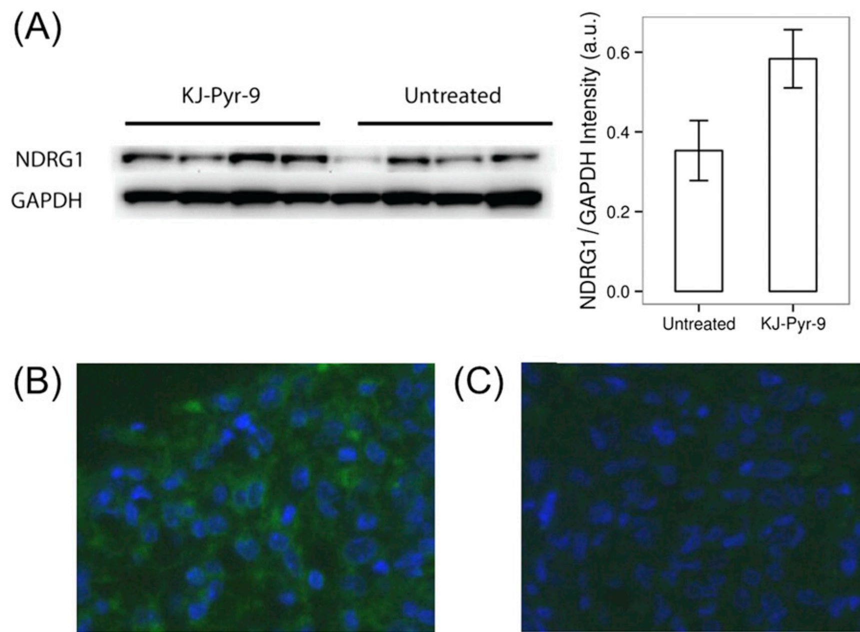

Fig. S6. KJ-Pyr-9–treated tumors show increased expression of NDRG1. (*A*) Higher but variable levels of NDRG1 are detected by Western blot. Quantification of GAPDH-normalized band intensity shows an increase in NDRG1 expression upon KJ-Pyr-9 treatment of xenograft tumors. a.u., arbitrary units. (*B* and *C*) Frozen sections of KJ-Pyr-9–treated (*B*) and untreated (*C*) tumors stained with an antibody directed against NDRG1. Error bars represent standard error of the mean (SEM).

Table S1. RNAseq of P493-6 cells: MYC signatures regulated by doxycycline and KJ-Pyr-9 analyzed by gene set enrichment analysis

Gene signatures of RNAseq (4)	NES	Nom *P* value	FDR *q* value
MYC signatures regulated by KJ-Pyr-9			
ODONNELL_TARGETS_OF_MYC_AND_TFRC_DN	−2.24	0	0
SCHUHMACHER_MYC_TARGETS_UP	−2.19	0	0
MENSSEN_MYC_TARGETS	−1.96	0	0.005
YU_MYC_TARGETS_UP	−1.82	0	0.016
SCHLOSSER_MYC_AND_SERUM_RESPONSE_SYNERGY	−1.68	0.009	0.041
BILD_MYC_ONCOGENIC_SIGNATURE	−1.64	0	0.051
SCHLOSSER_MYC_TARGETS_AND_SERUM_RESPONSE_UP	−1.61	0.011	0.066
KIM_MYC_AMPLIFICATION_TARGETS_UP	−1.54	0	0.092
DANG_REGULATED_BY_MYC_UP	−1.52	0.015	0.101
MYC signatures regulated by doxycycline			
SCHUHMACHER_MYC_TARGETS_UP	−3.75	0	0
SCHLOSSER_MYC_TARGETS_REPRESSED_BY_SERUM	−3.37	0	0
SCHLOSSER_MYC_TARGETS_AND_SERUM_RESPONSE_DN	−3.18	0	0
DANG_MYC_TARGETS_UP	−3.16	0	0
SCHLOSSER_MYC_TARGETS_AND_SERUM_RESPONSE_UP	−3.02	0	0
KIM_MYC_AMPLIFICATION_TARGETS_UP	−2.99	0	0
COLLER_MYC_TARGETS_UP	−2.94	0	0
MENSSEN_MYC_TARGETS	−2.94	0	0
ODONNELL_TARGETS_OF_MYC_AND_TFRC_DN	−2.93	0	0
DANG_REGULATED_BY_MYC_UP	−2.81	0	0
BILD_MYC_ONCOGENIC_SIGNATURE	−2.73	0	0
ACOSTA_PROLIFERATION_INDEPENDENT_MYC_TARGETS_UP	−2.68	0	0
YU_MYC_TARGETS_UP	−2.61	0	0
SCHLOSSER_MYC_AND_SERUM_RESPONSE_SYNERGY	−2.45	0	0
BENPORATH_MYC_TARGETS_WITH_EBOX	−2.12	0	0
ALFANO_MYC_TARGETS	−2.07	0	0
FERNANDEZ_BOUND_BY_MYC	−1.89	0	0.003
SCHLOSSER_SERUM_RESPONSE_AUGMENTED_BY_MYC	−1.8	0	0.006

FDR, false discovery rate; NES, normalized enrichment score; Nom, nominal.